Light diffusion through a turbid parallelepiped

Alwin Kienle

Institut für Lasertechnologien in der Medizin und Meßtechnik, Helmholtzstraße 12, D-89081 Ulm, Germany

Received January 21, 2005; accepted February 17, 2005

Solutions of the diffusion approximation to the radiative transport equation are derived for a turbid (rectangular) parallelepiped using the method of image sources and applying extrapolated boundary conditions. The derived solutions are compared with Monte Carlo simulations in the steady-state and time domains. It is found that the diffusion theory is in good agreement with Monte Carlo simulations provided that the light is detected sufficiently far from the incident beam. Applications of the derived solutions, including the determination of the optical properties of the turbid parallelepiped, are discussed. © 2005 Optical Society of America

OCIS codes: 170.0170, 170.3660, 170.4580, 170.5280, 170.6510, 290.1990.

1. INTRODUCTION

Theoretical models for the description of light propagation in turbid media are important in various scientific fields. In biomedical optics the necessity of these models is twofold. First, the knowledge of light penetration in tissue is relevant for therapeutical applications, and, second, such models are needed for determination of the optical properties of tissue as a prerequisite for many diagnostic applications. It is generally accepted that the transport theory correctly describes important quantities concerning light propagation in biological media.[1] However, no analytical solutions of the transport theory for relevant geometries are known. Thus, an approximation to the transport theory, the diffusion theory, is often applied, especially for the determination of the optical properties of tissue or whenever fast solutions are necessary.[1]

Several analytical solutions of the diffusion equation have been reported, for example, for the infinite and semi-infinite geometry in the time domain[2] and the steady-state domain.[3] Solutions for other geometries have been summarized by Arridge *et al.*[4] These authors showed that solutions of the diffusion equation can be easily derived from solutions for the conduction of heat. An analytical solution of the conduction of heat for a parallelepiped based on the eigenfunction method has been known for many decades.[5] Recently, the corresponding solution for the diffusion equation has been reported.[6] However, the sums involved in this solution converge slowly in the steady-state domain and for short times in the time domain.

In this study we present analytical solutions of the diffusion equation for a parallelepiped derived with the method of image sources, which converge much faster than the solution of the eigenfunction method and are easy to program. Solutions in the time and the steady-state domains are derived and compared with results obtained by the Monte Carlo method to investigate the validity of the diffusion equation. The Monte Carlo method is applied to solve numerically the transport equation and is used as reference for the performance of the solutions of the diffusion theory.

Potential applications of the derived solutions in the field of biomedical optics are, first, the *ex vivo* determination of the optical properties of biological tissue that cannot be prepared in geometries for which solutions of the diffusion equation are known, e.g., for small tissue samples like dentin or cartilage. Second, for certain *in vivo* measurements the parallelepiped might describe the real anatomy more accurately than the normally used geometrical models like slab geometry with lateral infinite extensions. Third, light penetration in *ex vivo* biological tissue is often demonstrated by illuminating a tissue block near an edge and measuring the light emitted from the lateral side. The solution presented here can be applied to describe these experiments accurately. For example, they can be used to obtain the optical properties of the investigated tissue. In addition, the derived solutions can be applied in other research fields for studying the propagation of light or other particles in random media as well as for deriving the corresponding solutions of the equation of heat conduction.

2. THEORY

In this section we derive the solution of the diffusion equation for a parallelepiped having the side lengths l_x, l_y, and l_z; see Fig. 1. A pencil beam is incident along the z direction perpendicular to the surface of the turbid medium at $(x_u, y_u, 0)$. It is assumed that all incident photons are initially scattered at (x_u, y_u, z_0), where $z_0 = (\mu_a + \mu_s')^{-1}$, and μ_s' and μ_a are the reduced scattering coefficient and the absorption coefficient, respectively. We employ the extrapolated boundary condition, which states that the fluence rate $\Phi(x, y, z)$ goes to zero at a distance

$$z_b = \frac{1 + R_{eff}}{1 - R_{eff}} 2D \tag{1}$$

beyond the actual surface; see Fig. 2. R_{eff} represents the fraction of the photons that is internally diffusely reflected at the boundary. It depends on the relative refractive index inside (n_i) and outside (n_o) the turbid medium.[7] $D = 1/(3\mu_s')$ is the diffusion coefficient. For the results shown in this paper we used $n_i = 1.50$ and $n_o = 1.33$ (representing dentin surrounded by water), from which follows

 © 2005 Optical Society of America

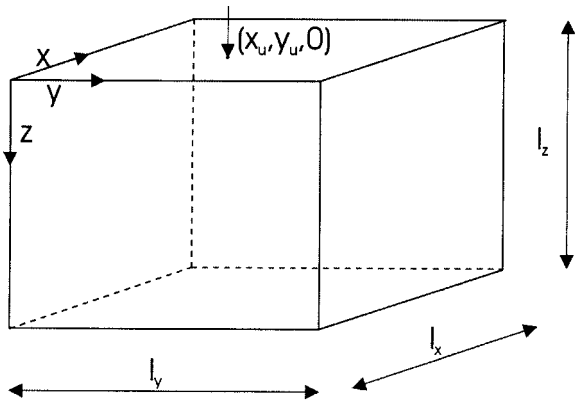

Fig. 1. Geometry of the (rectangular) parallelepiped used for the calculations.

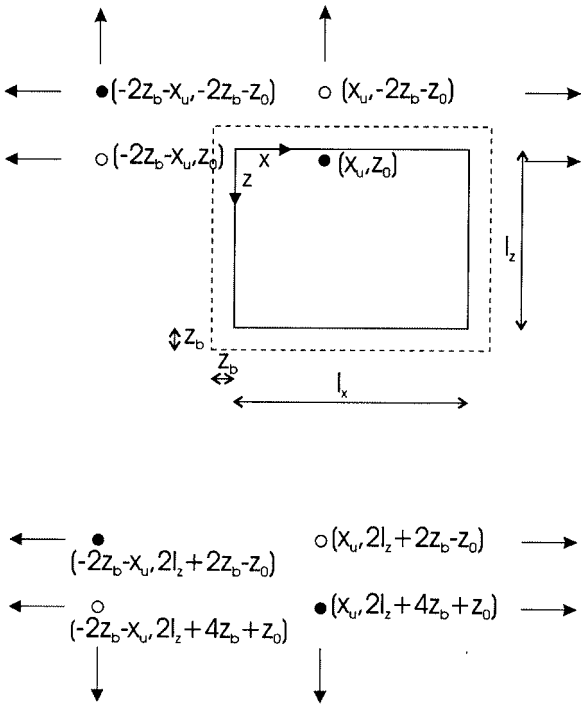

Fig. 2. Two-dimensional arrangement of the positive (solid circles) and negative (open circles) sources to fulfill the extrapolated boundary conditions. The four sources shown at the top of the figure are those for $l=0, n=0$, and the four sources at the bottom are those for $l=0, n=1$; see Eq. (5). The extrapolated boundaries are depicted by dashed lines. The arrows indicate that the point sources in each row are continued to infinity.

$R_{eff}=0.190$. First, the solution in the time domain is derived, then the solution in the steady-state domain. Finally, the applied Monte Carlo simulations are described.

A. Solution of the Diffusion Equation in the Time Domain

In the time domain the diffusion equation for the fluence rate $\Phi(\vec{r},t)$ is written

$$\frac{1}{c}\frac{\partial\Phi(\vec{r},t)}{\partial t} - D\nabla^2\Phi(\vec{r},t) + \mu_a\Phi(\vec{r},t) = S(\vec{r},t), \qquad (2)$$

where c is the speed of light in the turbid medium and $S(\vec{r},t)$ is the photon source, which is assumed to be an isotropic point source that emits an infinitely short light pulse at time $t=0$. In an infinite turbid medium the solution, which is simultaneously the Green's function for the problem considered, is[2]

$$\Phi(\vec{r},t) = \frac{c}{(4\pi Dct)^{3/2}}\exp(-\mu_a ct)\exp\left(-\frac{r^2}{4Dct}\right), \qquad (3)$$

where $r^2=(x-x_u)^2+(y-y_u)^2+(z-z_0)^2$. We recall the solution for a slab having lateral infinite extension to demonstrate how the extrapolated boundary conditions for a turbid parallelepiped can be fulfilled. In the case of the slab an infinite row of positive and negative sources in one dimension is used to satisfy the boundary conditions.[2] For a parallelepiped this procedure is extended to three dimensions. Thus an infinite three-dimensional grid of positive and negative point sources satisfies the boundary conditions at the six extrapolated plains. Figure 2 shows the distribution of these sources in two dimensions. We sum over all point sources using Eq. (3) to obtain the solution of the three-dimensional turbid parallelepiped as

$$\begin{aligned}\Phi(\vec{r},t) = \frac{c}{(4\pi Dct)^{3/2}}\exp(-\mu_a ct)\sum_{l=-\infty}^{\infty}\sum_{m=-\infty}^{\infty}\sum_{n=-\infty}^{\infty}\\ \times\Bigg[\exp\left(-\frac{(x-x_{1l})^2+(y-y_{1m})^2+(z-z_{1n})^2}{4Dct}\right)\\ -\exp\left(-\frac{(x-x_{1l})^2+(y-y_{1m})^2+(z-z_{2n})^2}{4Dct}\right)\\ -\exp\left(-\frac{(x-x_{1l})^2+(y-y_{2m})^2+(z-z_{1n})^2}{4Dct}\right)\\ +\exp\left(-\frac{(x-x_{1l})^2+(y-y_{2m})^2+(z-z_{2n})^2}{4Dct}\right)\\ -\exp\left(-\frac{(x-x_{2l})^2+(y-y_{1m})^2+(z-z_{1n})^2}{4Dct}\right)\\ +\exp\left(-\frac{(x-x_{2l})^2+(y-y_{1m})^2+(z-z_{2n})^2}{4Dct}\right)\\ +\exp\left(-\frac{(x-x_{2l})^2+(y-y_{2m})^2+(z-z_{1n})^2}{4Dct}\right)\\ -\exp\left(-\frac{(x-x_{2l})^2+(y-y_{2m})^2+(z-z_{2n})^2}{4Dct}\right)\Bigg],\end{aligned} \qquad (4)$$

where

$$x_{1l} = 2ll_x + 4lz_b + x_u,$$

$$x_{2l} = 2ll_x + (4l-2)z_b - x_u,$$

$$y_{1m} = 2ml_y + 4mz_b + y_u,$$

$$y_{2m} = 2ml_y + (4m-2)z_b - y_u,$$

$$z_{1n} = 2nl_z + 4nz_b + z_0,$$

$$z_{2n} = 2nl_z + (4n-2)z_b - z_0. \quad (5)$$

Equation (4) can be rewritten as follows:

$$\Phi(\vec{r},t) = \frac{c}{(4\pi Dct)^{3/2}}\exp(-\mu_a ct) \times \sum_{l=-\infty}^{\infty}\left[\exp\left(-\frac{(x-x_{1l})^2}{4Dct}\right) - \exp\left(-\frac{(x-x_{2l})^2}{4Dct}\right)\right] \times \sum_{m=-\infty}^{\infty}\left[\exp\left(-\frac{(y-y_{1m})^2}{4Dct}\right) - \exp\left(-\frac{(y-y_{2m})^2}{4Dct}\right)\right] \times \sum_{n=-\infty}^{\infty}\left[\exp\left(-\frac{(z-z_{1n})^2}{4Dct}\right) - \exp\left(-\frac{(z-z_{2n})^2}{4Dct}\right)\right]. \quad (6)$$

The time-resolved transmitted light from the side (L) and from the bottom (T) of the parallelepiped is calculated using Fick's law.[2] For example, in the latter case, using

$$T(x,y,t) = -D\frac{\partial}{\partial z}\Phi(x,y,z,t)|_{z=l_z}, \quad (7)$$

we get

$$T(x,y,t) = \frac{1}{2}(4\pi Dc)^{-3/2}t^{-5/2}\exp(-\mu_a ct) \times \sum_{l=-\infty}^{\infty}\left[\exp\left(-\frac{(x-x_{1l})^2}{4Dct}\right) - \exp\left(-\frac{(x-x_{2l})^2}{4Dct}\right)\right] \times \sum_{m=-\infty}^{\infty}\left[\exp\left(-\frac{(y-y_{1m})^2}{4Dct}\right) - \exp\left(-\frac{(y-y_{2m})^2}{4Dct}\right)\right] \times \sum_{n=-\infty}^{\infty}\left[(l_z-z_{1n})\exp\left(-\frac{(l_z-z_{1n})^2}{4Dct}\right) - (l_z-z_{2n}) \times \exp\left(-\frac{(l_z-z_{2n})^2}{4Dct}\right)\right]. \quad (8)$$

For $l_x = l_y = \infty$ only the terms of the first two sums that contain x_{10} and y_{10} are not zero. Thus from Eq. (8) follows the well-known solution of the time-resolved transmittance from a lateral infinite slab.[2,8] Similar to the solution for the slab geometry, Eq. (8) converges by evaluating only a few terms of the involved sums for typical optical and geometrical data found in biomedical optics. Thus the calculation time is only slightly longer than that needed for the solution of the slab geometry.

B. Solution of the Diffusion Equation in the Steady-State Domain

In the steady-state domain the diffusion equation becomes

$$D\nabla^2\Phi^s(\vec{r}) - \mu_a\Phi^s(\vec{r}) = -S^s(\vec{r}). \quad (9)$$

The steady-state quantities are marked by the superscript s. Assuming a steady-state point source at (x_u, y_u, z_0) the solution of the diffusion equation for an infinite medium is[3]

$$\Phi^s(r) = \frac{1}{4\pi D}\frac{\exp(-\mu_{eff}r)}{r}, \quad (10)$$

where $\mu_{eff} = (3\mu_a(\mu_a + \mu_s'))^{1/2}$. As in the time domain, the extrapolated boundary conditions for a parallelepiped can be fulfilled using a three-dimensional grid of point sources (see Fig. 2),

$$\Phi^s(x,y,z) = \frac{1}{4\pi D}\sum_{l=-\infty}^{\infty}\sum_{m=-\infty}^{\infty}\sum_{n=-\infty}^{\infty}\left(\frac{\exp(-\mu_{eff}r_1)}{r_1} - \frac{\exp(-\mu_{eff}r_2)}{r_2} - \frac{\exp(-\mu_{eff}r_3)}{r_3} + \frac{\exp(-\mu_{eff}r_4)}{r_4} - \frac{\exp(-\mu_{eff}r_5)}{r_5} + \frac{\exp(-\mu_{eff}r_6)}{r_6} + \frac{\exp(-\mu_{eff}r_7)}{r_7} - \frac{\exp(-\mu_{eff}r_8)}{r_8}\right), \quad (11)$$

where we used

$$r_1 = ((x-x_{1l})^2 + (y-y_{1m})^2 + (z-z_{1n})^2)^{1/2},$$

$$r_2 = ((x-x_{1l})^2 + (y-y_{1m})^2 + (z-z_{2n})^2)^{1/2},$$

$$r_3 = ((x-x_{1l})^2 + (y-y_{2m})^2 + (z-z_{1n})^2)^{1/2},$$

$$r_4 = ((x-x_{1l})^2 + (y-y_{2m})^2 + (z-z_{2n})^2)^{1/2},$$

$$r_5 = ((x-x_{2l})^2 + (y-y_{1m})^2 + (z-z_{1n})^2)^{1/2},$$

$$r_6 = ((x-x_{2l})^2 + (y-y_{1m})^2 + (z-z_{2n})^2)^{1/2},$$

$$r_7 = ((x-x_{2l})^2 + (y-y_{2m})^2 + (z-z_{1n})^2)^{1/2},$$

$$r_8 = ((x-x_{2l})^2 + (y-y_{2m})^2 + (z-z_{2n})^2)^{1/2}, \quad (12)$$

and the abbreviations of Eq. (5). Once again, Fick's law is applied to calculate the spatially resolved transmittance from the side (L^s) and from the bottom (T^s). For the latter case using

$$T^s(x,y) = -D\frac{\partial}{\partial z}\Phi(x,y,z)|_{z=l_z}, \quad (13)$$

we have

$$T^s(x,y) = \frac{1}{4\pi}\sum_{l=-\infty}^{\infty}\sum_{m=-\infty}^{\infty}\sum_{n=-\infty}^{\infty}\left((l_z-z_{1n})(\mu_{eff}+1/r_1) \times \frac{\exp(-\mu_{eff}r_1)}{r_1^2} - (l_z-z_{2n})(\mu_{eff}+1/r_2) \times \frac{\exp(-\mu_{eff}r_2)}{r_2^2} - (l_z-z_{1n})(\mu_{eff}+1/r_3) \times \frac{\exp(-\mu_{eff}r_3)}{r_3^2} + (l_z-z_{2n})(\mu_{eff}+1/r_4)\right)$$

$$\times \frac{\exp(-\mu_{eff} r_4)}{r_4^2} - (l_z - z_{1n})(\mu_{eff} + 1/r_5)$$

$$\times \frac{\exp(-\mu_{eff} r_5)}{r_5^2} + (l_z - z_{2n})(\mu_{eff} + 1/r_6)$$

$$\times \frac{\exp(-\mu_{eff} r_6)}{r_6^2} + (l_z - z_{1n})(\mu_{eff} + 1/r_7)$$

$$\times \frac{\exp(-\mu_{eff} r_7)}{r_7^2} - (l_z - z_{2n})(\mu_{eff} + 1/r_8)$$

$$\times \frac{\exp(-\mu_{eff} r_8)}{r_8^2}\Bigg), \tag{14}$$

where in the r_i terms of Eq. (12), z has to be replaced by l_z. We note that for calculation of the spatially resolved reflectance the use of an additional term proportional to the fluence rate in Eq. (13) improves the accuracy of the results obtained.[9]

For $l_x = l_y = \infty$ only the terms that contain r_1 and r_2 are not zero in Eq. (12), yielding the solution of the steady-state spatially resolved transmittance from a slab.[10] In general, Eq. (12) converges fast for typical parameters used in biomedical optics. However, a larger number of terms has to be calculated if the absorption coefficient is exceptionally small ($\mu_a \approx 0.001$ mm^{-1}).

C. Monte Carlo Simulations

To investigate the validity of the diffusion theory for a parallelepiped, the derived solutions are compared with Monte Carlo simulations. The Monte Carlo method has been described in detail elsewhere.[11] The salient features of our code are as follows. The light beam is incident perpendicularly on the top side of the parallelepiped at $(x_u, y_u, 0)$. We apply a Henyey–Greenstein function as phase function using an anisotropy factor of $g = 0.9$ for the simulations in the steady-state domain. This value of g is close to those found in biological tissue. For the calculations in the time domain an anisotropy factor of $g = 0.8$ was used to accelerate the simulations. The difference in the refractive index outside and inside the parallelepiped is considered by applying Fresnel equations at the six sides of the cube.[11]

The accuracy of the Monte Carlo code was thoroughly tested. For example, the beam was incident at different sides of the cube and the spatially resolved transmittance obtained from opposite sides was compared. The results were found to be the same within the statistics of the simulations.

3. RESULTS

The solutions derived in Section 2 are compared with Monte Carlo simulations in the time domain (Subsection 3.A) and in the steady-state domain (Subsection 3.B). A cube was used as the geometry of the turbid media for all calculations shown in this paper. We note that similar results were obtained for a general parallelepiped. The solutions for a cube were obtained from the equations presented in Section 2 by setting $l_x = l_y = l_z = l_c$, where l_c is the cube's side length. The following optical properties, which are typical for biological tissue, were used for the presented results. The reduced scattering coefficient was chosen as $\mu_s' = 1$ mm^{-1} and the absorption coefficient as $\mu_a = 0.01$ mm^{-1}.

A. Calculations in the Time Domain

In Fig. 3 the time-resolved transmittance from a cube calculated with the Monte Carlo method (noisy curves) is compared with the solution of the diffusion equation [Eq. (8), dashed curves]. The side length of the cube is $l_c = 19$ mm. The light beam is incident on the middle of the cube's top side at $(l_c/2, l_c/2, 0)$, and the time-resolved transmittance is calculated at the middle of the bottom side at $(l_c/2, l_c/2, l_c)$. For comparison $T(t)$ is also shown for a slab having a thickness of $d = 19$ mm and infinite lateral extension. At early times large differences can be seen due to the well-known breakdown of the diffusion approximation. At maximum values of $T(x, y)$ the diffusion theory underestimates and at long time values it overestimates slightly the Monte Carlo data. This general behavior is similar for the slab geometry, but the differences between diffusion theory and Monte Carlo simulations are a bit smaller. This is expected because the volume of the cube is smaller than that of the slab and thus the diffusion approximations is worse, because the transmitted photons have experienced fewer scattering interactions. In addition Fig. 3 demonstrates that large errors would have been made if the slab geometry had been applied to describe the light propagation in a cube for the physical parameters used in the presented calculations.

Figure 4 shows results from calculations analogous to Fig. 3, but the side length of the cube is now reduced to $l_c = 9$ mm. The same general features as described above can be observed. However, the relative differences between the diffusion equation and the Monte Carlo simulations are now larger due to the smaller volume of the cube.

Calculations with different optical coefficients were performed (results not shown). Generally, as expected, it was found that the accuracy of the diffusion equation is only slightly influenced by the applied absorption coefficient as long as $\mu_a \ll \mu_s'$, whereas larger values of the reduced scattering coefficients increased its accuracy. The latter can also be seen by comparing Fig. 4 with Fig. 3. Increasing the scattering coefficient for the calculations in Fig. 4 by a factor of approximately two leads to results with differences similar to those shown in Fig. 3 due to scaling principles. We also found that, similar to the case of slab geometry, the relative difference of the refractive indices inside and outside the turbid medium has a relatively strong influence on the performance of the diffusion theory. The accuracy of the diffusion theory is best for matched refractive index and gets worse for larger relative differences of the refractive index.

B. Calculations in the Steady-State Domain

Figure 5 shows the steady-state spatially resolved transmittance from the bottom and from the lateral side of a cube with a side length of $l_c = 5$ mm calculated with the diffusion theory (solid curve) and with the Monte Carlo method (circles). The light beam is incident at the middle

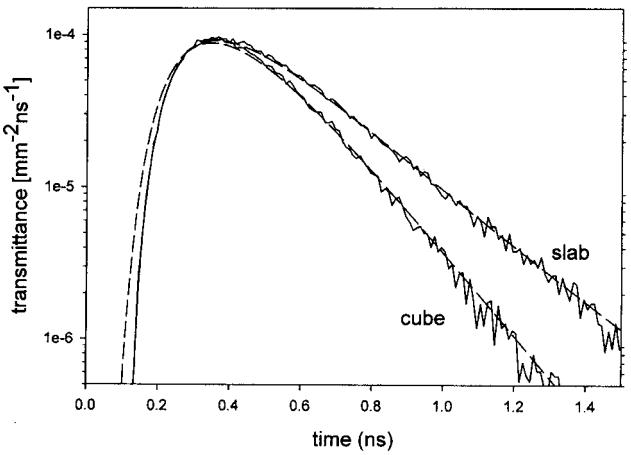

Fig. 3. Comparison of the time-resolved transmittance from a cube (l_c=19 mm) and from a slab (d=19 mm) calculated with the diffusion theory (dashed curves) with Monte Carlo simulations (solid curves).

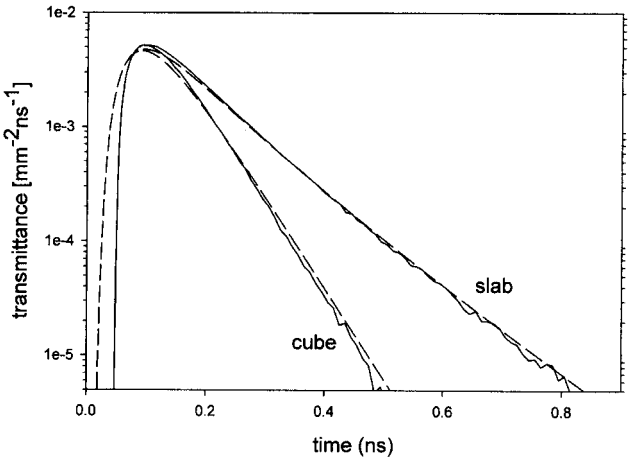

Fig. 4. Comparison of the time-resolved transmittance from a cube (l_c=9 mm) and from a slab (d=9 mm) calculated with the diffusion theory (dashed curves) with Monte Carlo simulations (solid curves).

of the top side $(l_c/2, l_c/2, 0)$. The transmittance from the bottom side, T^s, is shown versus the distance from the middle of the bottom side in the direction of the negative x axis, i.e., from $(l_c/2, l_c/2, l_c)$ to $(0, l_c/2, l_c)$; see inset of Fig. 5. The transmittance from the lateral side, L^s, is shown versus the distance from $(0, l_c/2, 0)$ in the direction of the positive z axis; see inset of Fig. 5. As can be seen in Fig. 5, the equations derived from the diffusion theory are close to the Monte Carlo simulations, even for the small cube with l_c=5 mm. Remembering Fig. 4, this seems surprising at first sight, because there the relative accuracy of the diffusion theory is worse, although the cube is larger. This can be explained by the features of the time-resolved transmittance shown in subsection 3.A, because $T(t)$ calculated from diffusion theory is for certain times larger and for other times smaller than the Monte Carlo simulations. Thus for the steady-state solution, which is equal to the integration of the time-resolved transmittance, these differences cancel out. In general, we recommend checking the accuracy of the diffusion equation in the steady-state domain for the considered geometrical and optical parameters by comparison with Monte Carlo simulations when the volume of the parallelepiped is small.

Figure 6 shows a comparison of the steady-state spatially-resolved transmittance from the lateral side of a cube with side lengths of l_c=41 mm calculated with the diffusion theory (dashed curves) to Monte Carlo simulations (solid curves). In contrast to Fig. 5, the light beam is not incident in the middle but near the edge of the cube's top side, at $(1\text{ mm}, l_c/2, 0)$ and $(3\text{ mm}, l_c/2, 0)$. The transmittance from the lateral side, L^s, is shown versus the distance from $(0, l_c/2, 0)$ in the direction of the positive z axis; see inset of Fig. 6. In the case where the incident beam is 1 mm distant from the edge of the cube's top side, the accuracy of the diffusion theory is poor for small distances due to the small number of scattering interactions

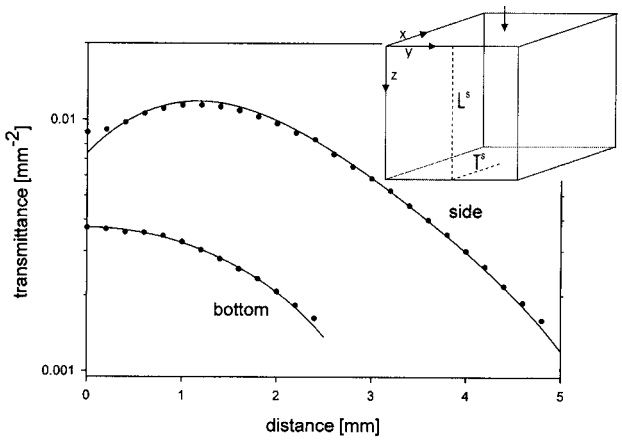

Fig. 5. Comparison of the spatially resolved transmittance from the bottom and the lateral side of a cube (l_c=9 mm) calculated by the diffusion theory (solid curves) with Monte Carlo simulations (circles). The light beam is incident on the middle of the cube's top side. The dashed lines in the inset give the location of the measurement of the transmittance from the lateral side, L^s, and from the bottom side, T^s.

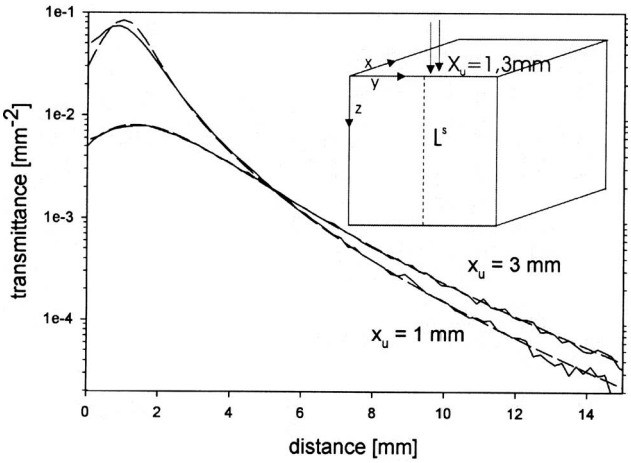

Fig. 6. Comparison of the spatially-resolved transmittance from the lateral side of a cube (l_c=41 mm) calculated by the diffusion theory (dashed curves) with Monte Carlo simulations (solid curves). The light beam is incident 1 mm and 3 mm away from the edge of the cube's top side. The dashed line in the inset gives the location of the measurement of the transmittance, L^s.

of the photons transmitted at these distances. However, for larger distances and for the whole curve calculated for a light beam incident at 3 mm from the edge, the diffusion theory matches well the results of the Monte Carlo simulations.

4. CONCLUSIONS

A solution of the diffusion theory for light propagation in turbid media has been derived for a parallelepiped using the extrapolated boundary condition. In the literature a solution using the method of eigenfunctions has been reported.[5,6] However, the sums involved in this solution converge slowly in the steady-state domain and for short times in the time domain, whereas the solution proposed in this study converges much faster. It is based on the method of image sources and is a three-dimensional extension of the one-dimensional case that has been already used for the derivation of the solution for a slab geometry.[2] It can also be shown that both solutions, that derived with the method of eigenfunctions and that obtained with the method of image sources, are identical using a theorem given in the book of Carslaw and Jaeger [5] (page 275). We note that Barnett, independently of us, recently mentioned the possibility of deriving the solution of the diffusion equation for a parallelepiped using the method of image sources.[12] We also note that the deduced solutions can be used to obtain the corresponding solutions of the equation of conduction of heat.

The solutions derived from the diffusion equation were compared to Monte Carlo simulations in the steady-state and in the time domains. In general, these solutions are close to Monte Carlo simulations, if the detected photons are in the diffusive regime, i.e., sufficiently far from the incident beam. It was shown that in the steady-state domain the accuracy of the diffusion theory is good even for relative small volumes; see Fig. 5. For this case (l_c $=5$ mm, $n_i=1.5$, $n_o=1.33$) we investigated the inverse problem, the determination of the optical properties (data not shown). We fitted the steady-state solution of the diffusion equation to Monte Carlo simulations that were calculated for a range of typical values of the absorption and the reduced scattering coefficients to be found in biological tissue. The spatially resolved transmittance from the bottom and from the lateral side were simultaneously fitted. We found that the errors of the reduced scattering coefficient obtained were smaller than 10%, whereas the average error of the derived absorption coefficient was about 30%.

Finally, we calculated the spatially resolved transmittance from the lateral side of a large cube ($l_c=41$ mm), which was illuminated by a light beam incident on the top side close to the edge. This arrangement is often used to demonstrate the light penetration in *ex vivo* biological tissue. Figure 6 shows that the spatially resolved transmittance curves obtained depend strongly on the distance of the laser beam from the edge. Thus for the interpretation and evaluation of these measurements, theoretical models are necessary. In addition, these measurements allow one to obtain the optical properties of the involved tissues using the derived solutions.

The author's e-mail address is alwin.kienle@ilm.uni-ulm.de.

REFERENCES

1. A. Ishimaru, *Wave Propagation and Scattering in Random Media* (Academic, 1978).
2. M. S. Patterson, B. Chance, and B. C. Wilson, "Time resolved reflectance and transmittance for the noninvasive measurement of tissue optical properties," Appl. Opt. **28**, 2331–2336 (1989).
3. T. J. Farrell, M. S. Patterson, and B. C. Wilson, "A diffusion theory model of spatially resolved, steady-state diffuse reflectance for the noninvasive determination of tissue optical properties *in vivo*," Med. Phys. **19**, 879–888 (1992).
4. S. R. Arridge, M. Cope, and D. T. Delpy, "The theoretical basis for the determination of optical pathlength in tissue: temporal and frequency analysis," Phys. Med. Biol. **37**, 1531–1560 (1992).
5. H. S. Carslaw and J. C. Jaeger, *Conduction of Heat in Solids*, (Clarendon, 1959).
6. F. Martelli, A. Sassaroli, S. Del Bianco, Y. Yamada, and G. Zaccanti, "Solution of the time-dependent diffusion equation for layered diffusive media by the eigenfunction method," Phys. Rev. E **67**, 056623-1–14 (2003).
7. R. C. Haskell, L. O. Svaasand, T. T. Tsay, T. C. Feng, M. McAdams, and B. J. Tromberg, "Boundary conditions for the diffusion equation in radiative transfer," J. Opt. Soc. Am. A **11**, 2727–2741 (1994).
8. D. Contini, F. Martelli, and G. Zaccanti, "Photon migration through a turbid slab described by a model based on diffusion approximation. I. Theory," Appl. Opt. **36**, 4587–4599 (1997).
9. A. Kienle and M. S. Patterson, "Improved solutions of the steady-state and the time-resolved diffusion equations for reflectance from a semi-infinite turbid medium," J. Opt. Soc. Am. A **14**, 246–254 (1997).
10. A. Kienle and R. Steiner, "Determination of the optical properties of tissue by spatially resolved transmission measurements and Monte Carlo simulations," Proc. SPIE **2077**, 142–152 (1993).
11. T. J. Pfefer, J. K. Barton, E. K. Chan, M. G. Ducros, B. S. Sorg, T. E. Milner, J. S. Nelson, and A. J. Welch, "A three-dimensional modular adaptable grid numerical model for light propagation duing laser irradiation of skin tissue," IEEE J. Sel. Top. Quantum Electron. **2**, 934–942 (1996).
12. A. H. Barnett, "A fast numerical method for time-resolved photon diffusion in general stratified turbid media," J. Comput. Phys. **201**, 771–797 (2004).